International Journal of Minerals, Metallurgy and Materials
Volume 19, Number 3, Mar 2012, Page 266
DOI: 10.1007/s12613-012-0549-7

Synthesis of $NiCr_2O_4$ spinel coatings with high emissivity by plasma spraying

Zhen-qi Zhu[1)], *Xu-dong Cheng*[2)], *Wei-ping Ye*[1)], *and Jie Min*[2)]

1) School of Materials Science and Technology, Wuhan University of Technology, Wuhan 430070, China

2) State Key Laboratory of Advanced Technology for Materials Synthesis and Processing, Wuhan University of Technology, Wuhan 430070, China

(Received: 21 February 2011; revised: 12 May 2011; accepted: 20 May 2011)

Abstract: Air plasma spraying (APS) was used to produce high emissivity coatings with a $NiCr_2O_4$ spinel structure. The relationship between the emissivity and the crystal structure was investigated. X-ray diffraction (XRD) analyses show that $NiCr_2O_4$ spinel has been fabricated with the space group *Fd*3*m*. Scanning electron microscope (SEM) photographs show that the coating consists of a laminated structure with homogeneous grains and high porosity because of the unique feature of plasma spraying. The emissivity measurement and Fourier transformation infrared radiation (FT-IR) spectra show that $NiCr_2O_4$ has a high emissivity of about 0.91 because of its special spinel structure. APS is a suitable method to produce high emissivity coatings.

Keywords: infrared radiation; coatings; plasma spraying; emissivity; crystal structure; industrial furnaces

1. Introduction

High emissivity coatings used at high temperature are attracting great attention because of their significant energy saving in industrial furnaces. Composite coatings such as SiC-Si_3N_4-Al_2O_3 [1], ZrO_2-Cr_2O_3-SiC [2], and Al_2O_3-SiO_2 [3] have been successfully produced by brush methods with a high emissivity. However, both the kind and the performance of these coatings are still limited [4]. Especially, the adhesion strength of these coatings is generally weak. Besides, the correlation between their microstructure and radiation property still needs a great deal research. Recently, Cu-Mn-Co-Cu-O spinel has been found to have a high emissivity of 0.92 [5].

On the other hand, $NiCr_2O_4$ spinel has been investigated by several researchers due to its versatile applications such as in chemical industrial fields [6] and electronic apparatus [7]. However, the infrared radiation property of $NiCr_2O_4$ structure has not been studied in detail. Thanks to the high emissivity of NiO and Cr_2O_3, $NiCr_2O_4$ might have high emissivity as well as the spinel compound mentioned above.

The air plasma spraying (APS) technique is an economical and effective method to produce functional coatings such as thermal barrier coatings [8], abradable sealing coatings [9], and wear-resistance coatings [10]. Above all, it is a versatile tool to fabricate most materials on various substrates with good adhesion strength. Moreover, it is very convenient to produce a porous coating with controllable thickness, which is favorable for the enhancement on emissivity. However, the preparation of high radiation coatings by APS method has not been reported so far.

The purpose of the present work is to fabricate high emissivity coatings with a $NiCr_2O_4$ spinel structure on a copper sheet by APS method and study the relationship between the emissivity and the crystal structure. To characterize these coatings, X-ray diffraction (XRD), scanning electron microscopy (SEM), Fourier transformation infrared radiation (FT-IR), and infrared radiation property measurements were performed.

2. Experimental

The preparation for high emissivity coatings involves two stages mainly, spray drying and plasma spraying. At first, raw materials including metal oxides (Cr_2O_3, NiO, TiO_2, Al_2O_3, SiO_2, and Fe_2O_3), organic binder, and deionized water were mixed in a proportion to become a well-ground

Corresponding author: Zhen-qi Zhu E-mail: hubeizhq@163.com

slurry. Then, in the spray dry tower, the slurry was sprayed to agglomerated powder. Before plasma spraying, the sprayed powder was baked for 4 h at 500, 900, 1000, and 1200°C (numbered as samples a, b, c, and d, respectively). The APS equipment was a plasma-spraying system (GP-80, Jiujiang Spray Equipment Corporation, China). Prior to APS $NiCr_2O_4$ coatings, a Ni/Al bond coating with a thickness of 80 μm was deposited on the substrate. At last, coatings with an overall thickness of 0.3 mm were deposited on the rectangle copper sheet (150 mm × 100 mm). The typical operating condition is listed in Table 1.

Table 1. Plasma spraying parameters

Parameters	Values
Arc voltage and current / V	80
Arc current / A	550
Powder feed rate / ($g \cdot min^{-1}$)	25-35
Spray distance / mm	70-100
Plasma gas flow / ($m^3 \cdot h^{-1}$)	0.8
Powder size / μm	45-75

The phase structure was identified from XRD patterns using an X-ray diffractometer (Model D/MAXIII, Rigaku, Japan) at a scanning speed of 0.02°/s. Microstructures of these coatings were observed by using a JSM-5610LV SEM. The infrared radiation characteristics were examined using an infrared radiation instrument (Model IRE-2, China) at 600°C. The total emissivity was calculated by integrating the emissivity in the whole bands. The FT-IR spectra were measured on a Nicolet 60-SXB FT-IR spectrometer (resolution 0.02 cm^{-1}) over a spectral range of 400 to 4000 cm^{-1}.

3. Results and discussion

3.1. Thermodynamic analysis

To determine possible products during the experiment, thermodynamics analysis was employed before the experiment. At first, the phase diagram of Cr_2O_3-NiO was observed to determine an appropriate baking temperature. From the diagram, beyond 2000°C, mixture powders can transform into liquid phase. Hence, the preparatory range of baking temperature was about 1700 to 1800°C according to the experience of solid-phase synthesis. Secondly, the Gibbs free energy changes ΔG involved in each reaction were calculated as a function of temperature and plotted in Fig. 1. The standard molar Gibbs free energy of $NiCr_2O_4$ agreed with that of Rudnyi [11]. In particular, $NiCr_2O_4$ was the major product due to the lowest ΔG, which was also one reason why we chose $NiCr_2O_4$ among those AB_2O_4 spinel compounds. Moreover, with increasing temperature, the trend of the forward reaction ($NiO + Cr_2O_3 \rightarrow NiCr_2O_4$) decreased according to the ΔG curve. This suggested that an excessive temperature may reduce the production of $NiCr_2O_4$ spinel. The baking temperature range was chosen to be 900 to 1200°C in the end.

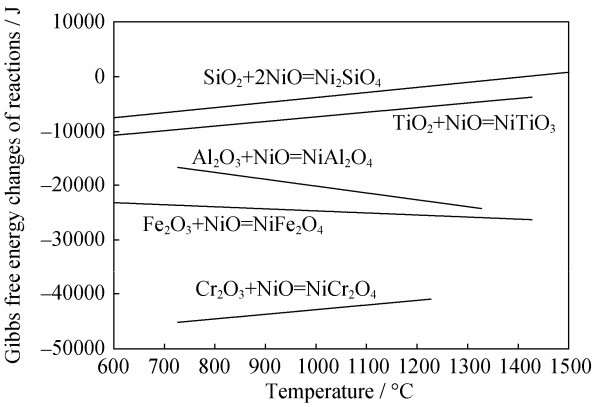

Fig. 1. Gibbs free energy changes of reactions corresponding to different temperatures.

3.2. XRD patterns

The XRD patterns of coating samples using the feedstock powders baked at different temperatures are shown in Fig. 2. It indicated that the samples were crystalline and identified as a mixture of oxides due to those sharp diffraction peaks. Some unmarked peaks were probably corresponding to minor TiO_2, Al_2O_3, SiO_2, or Fe_2O_3. In sample a, except NiO and Cr_2O_3, no spinel structure was found. It implied that when the baking temperature was too low, the powders could not react with each other. Furthermore, the spraying time was too short (10^{-2}-10^{-5} s) to start the reaction despite of high temperature. However, once powders were baked

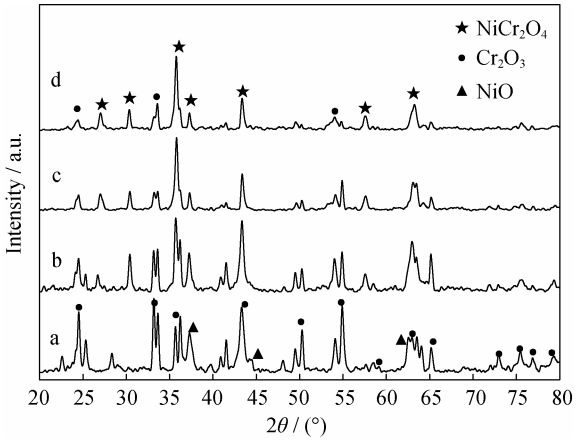

Fig. 2. XRD patterns of the coatings using the feedstock powders baked at different temperatures: a—500°C; b—900°C; c—1000°C; d—1200°C.

at beyond 900°C, $NiCr_2O_4$ spinel was successfully generated. As shown in Fig. 2, those diffraction peaks were fully consistent with the standard JCPDS cards of $NiCr_2O_4$ (No. 89-6615), Cr_2O_3 (No. 84-1616), and NiO (No. 89-5881), respectively. Moreover, with raising temperature, the intensity of Cr_2O_3 and NiO peaks decreased but $NiCr_2O_4$ peaks increased. Particularly, it was surprising for us to find that sample d mainly consisted of $NiCr_2O_4$ and Cr_2O_3 but without trace of NiO. This suggested that adequate reaction between raw materials led to more NiO consumed than Cr_2O_3. The result was different from the conclusion of Rudnyi *et al.* [11]. They reckoned that the activity of NiO was equal to that of Cr_2O_3. In fact, it was only a theoretical condition achieved by equilibrium state. Additionally, Sloczynski *et al.* [5] prepared $NiCr_2O_4$ spinel by a coprecipitation method using a solution of nickel and chromium nitrates as raw material. Being a wet chemical method, it took a long time (over 50 h) and a complex procedure. In contrast, the solid-phase synthesis was very simple and effective. As will be discussed later, owing to the cubic structure (space group: *Fd*3*m*), $NiCr_2O_4$ has a high emissivity close to 0.91.

3.3. Morphology observation

Coating thickness and surface morphology (such as roughness, porosity, and particle size) have an important role in determining the coating emissivity. Fig. 3 shows the surface structure view of the as-prepared coating. It was very rough and porous, which was composed of a laminated structure with homogeneous grains. Due to the fact that starting powders had different densities, sizes, morphologies, melting temperatures, and flow abilities, the layers contained some inhomogeneities such as fluctuation and porosity. These morphology features may be explained by the "layer-by- layer" model proposed by Ng *et al.* [12]. Yu *et al.* [13] proposed a theoretical model to interpret the effect of porosity on emissivity. According to their results, porosity is helpful for high emissivity. Tang *et al.* [14] confirmed that high roughness increases directional emissivity on the basis of the radiation theory. As for coating thickness, a critical thickness is necessary for achieving high emissivity in light of different coating compositions. Over this thickness, the emissivity almost does not change [4]. Therefore, APS is an effective tool to produce a high emissivity coating because the coating produced by APS usually has high porosity, roughness, and controllable thickness. To our knowledge, more coatings with high emissivity would be produced by combining the spinel structure with APS together in the future.

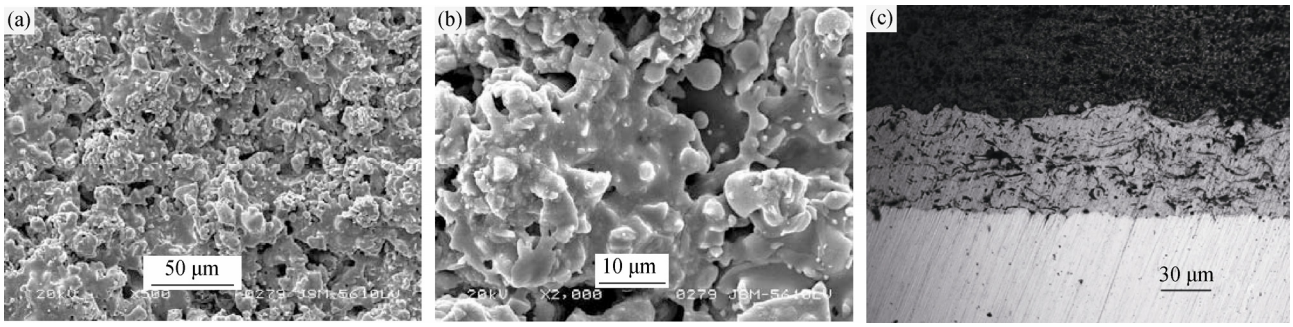

Fig. 3. Images of the as-prepared coating using the feedstock powders baked at 900°C: (a) low magnification; (b) high magnification; (c) cross-sectional image.

3.4. Emissivity performance

Fig. 4 gives the total emissivity of the samples baked at 600°C using the feedstock powders baked at different temperatures. As shown in Fig. 4, it can be seen that sample c has the maximum value (0.91), which may indicate that $NiCr_2O_4$ spinel has a larger emissivity than NiO (0.89) and Cr_2O_3 (0.83). Thus, when baking at low temperature (i.e., 500°C), without $NiCr_2O_4$ spinel formation, the emissivity is the smallest. However, with the baking temperature increasing, the emissivity of the samples increases first but then decreases after 1000°C lightly. Actually, the coating emissivity is determined by many factors such as chemical composition, crystal structures, chemical bonding, impurities, surface parameters, and the type of lattice defects. These factors play a complex and flexible role in influencing the emissivity. For example, composite materials can improve surface emissivity. Sample b was a mixture of $NiCr_2O_4$, NiO, and Cr_2O_3, with the minimum content of spinel, while sample d has a lower content of Cr_2O_3 with the maximum content of spinel. Even though sample d had more $NiCr_2O_4$ than sample c, the emissivity declined on the contrary due to the shortage of NiO. Accordingly, the highest content of $NiCr_2O_4$ may not mean the highest emissivity. Nevertheless, it still can prove that the $NiCr_2O_4$ coating with a spinel structure has a high emissivity of about 0.91 as presumed before indeed. Considering the stability at high tem-

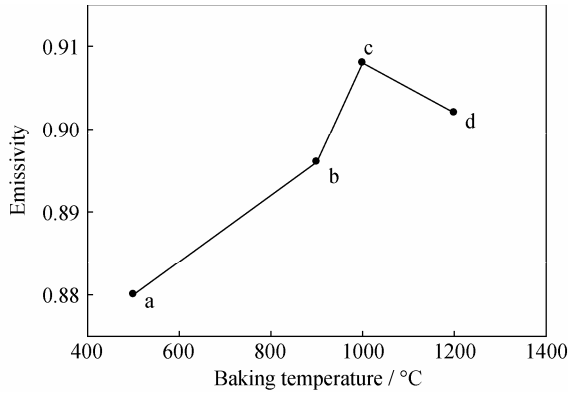

Fig. 4. Relationship between emissivity and baking temperature.

perature, we may predict that $NiCr_2O_4$ will have a wide application prospect. Furthermore, other spinel compounds probably also have high emissivity profiting from their spinel structure likewise.

3.5. FT-IR measurement

The emissivity of $NiCr_2O_4$ coatings is associated with the symmetrical characteristic of microstructure, which is characterized by the infrared spectra technique. In most literatures, the infrared spectra of AB_2O_4 spinel are interpreted as vibrations of the $A–O_4$ tetrahedron and $B–O_6$ octahedron. Fig. 5 shows the infrared absorption spectra of the samples in the range of 4000 to 400 cm^{-1}. In order to mark these bands, the spectra of NiO, Cr_2O_3, and AB_2O_4 spinel were checked over carefully. NiO has typical bands at 410, 445, and 490 cm^{-1} corresponding to the Ni–O stretching vibration [15-16]. Cr_2O_3 has typical bands at 545 and 720 cm^{-1}, corresponding to the Cr–O stretching vibration [17-18]. Based on these data, sample a is a simple mixture of NiO and Cr_2O_3. With the baking temperature increasing, the typical absorption bands belonging to the spinel structure appeared in samples b to d, as shown in Fig. 5(a). These results were consistent with XRD analysis completely. Additionally, the bands at 3455 and 1641 cm^{-1} in Fig. 5(b) were assigned to the O–H stretching and bending vibration of adsorbed water, respectively [19].

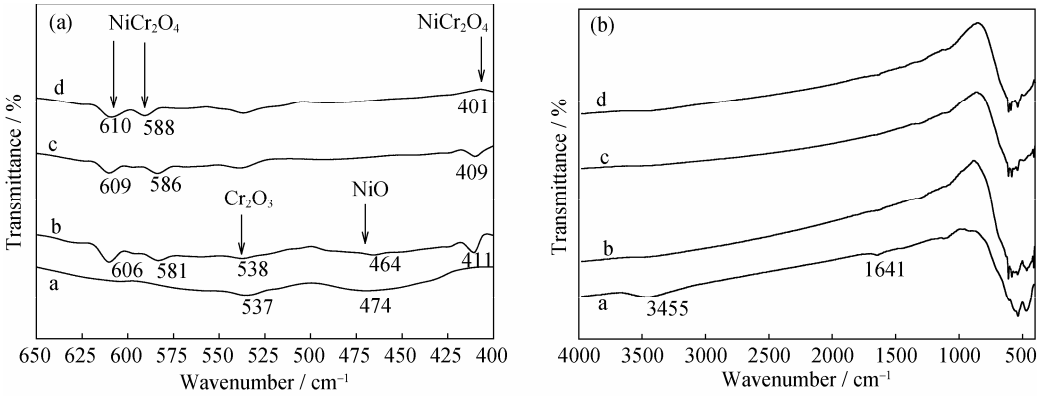

Fig. 5. FT-IR spectra of the samples: (a) bands at 400 to 625 cm^{-1}; (b) bands at 4000 to 400 cm^{-1}.

As for the spectra of spinel compounds, the group theory predicts that four infrared active vibrations should be present according to the factor-group approximation [20]. Two intense bands are at 700 to 400 cm^{-1}, and the other two at the low frequency of 300 to 200 cm^{-1}, but the latter is generally difficult to record. Two absorption bands appearing at 610 and 400 cm^{-1} are attributed to the stretching vibration of the Cr–O bond in tetrahedral and octahedral groups, respectively [21]. But recently, it tends to be accepted that complex vibrations of the entire lattice are the atomic displacement contributing to the infrared spectra of spinel phases. Moreover, the absorption bands vary considerably from a compound to another compound, depending on the masses, charges, and chemical properties of the ions. According to the symmetry theory, the lower symmetry of vibration will lead to a larger change of molecular transition dipoles, resulting in high emissivity. Thanks to the complicated structure of spinel, it has numerous vibration modes. As result, high emissivity has been achieved owing to the spinel structure.

4. Conclusion

High emissivity coatings with a spinel structure ($NiCr_2O_4$) have been fabricated by APS. An appropriate baking temperature range of 900 to 1200°C is necessary for the preparation of $NiCr_2O_4$ spinel. APS is a suitable method to fabricate high emissivity coatings, because the coatings generally have a rough and porous surface. The high emissivity of about 0.91 is mainly attributed to the spinel structure, which is very useful for the application at high temperature. However, further work will be required to find the relationship between emissivity and microstructure for $NiCr_2O_4$ spinel.

Acknowledgements

Authors would like to thank Yu Zeng and Ping Ye of China National Infrared & Industrial Electrothermal Products Quality Supervision & Testing Centre for the infrared normal total emissivity measurements of the coatings.

References

[1] M. Falz and G. Leonhardt, PVD coatings with high IR emissivity for high temperature applications of Co-based alloys, *Surf. Coat. Technol.*, 61(1993), p.97.

[2] Z.G. Dan, D.Q. Cang, H.M. Zhou, *et al.*, Microstructure and properties of high emissivity coatings, *J. Univ. Sci. Tech. Beijing,* 15(2008), No.5, p.627.

[3] K. Shimazaki, M. Imaizumi, and K. Kibe, SiO_2 and Al_2O_3/SiO_2 coatings for increasing emissivity of Cu(In, Ga)Se_2 thin-film solar cells for space applications, *Thin Solid Films,* 516(2008), p.2218.

[4] Y. Zhang and D.J. Wen, Relationship between infrared radiation and crystal structure in Fe-Mn-Co-Cu-O spinels, *Acta Metall. Sin. Engl. Lett.*, 21(2008), p.15.

[5] X.D. He, Y.B. Li, L.D. Wang, *et al.*, High emissivity coatings for high temperature application: progress and prospect, *Thin Solid Films*, 517(2009), p.5120.

[6] J. Słoczyński, J. Ziółkowski., B. Grzybowska, *et al.*, Oxidative dehydrogenation of propane on $Ni_xMg_{1-x}Al_2O_4$ and $NiCr_2O_4$ spinels, *J. Catal.*, 187(1999), p.410.

[7] S. Zhuiykov, T. Nakano, A. Kunimoto, *et al.*, Potentiometric NO_x sensor based on stabilized zirconia and $NiCr_2O_4$ sensing electrode operating at high temperatures, *Electrochem. Commun.*, 3(2001), p.97.

[8] M. Gell, L.D. Xie, E.H. Jordan., *et al.*, Mechanisms of spallation of solution precursor plasma spray thermal barrier coatings, *Surf. Coat. Technol.,* 188(2004), p.101.

[9] H.I. Faraoun, T. Grosdidier, J.L. Seichepine, *et al.*, Improvement of thermally sprayed abradable coating by microstructure control, *Surf. Coat. Technol.*, 201(2006), p.2303.

[10] E.P. Song, J. Ahn, S. Lee, *et al.*, Effects of critical plasma spray parameter and spray distance on wear resistance of Al_2O_3-8 wt.%TiO_2 coatings plasma-sprayed with nanopowders, *Surf. Coat. Technol.*, 202(2008), p.3625.

[11] E.B. Rudnyi, E.A. Kaibicheva, L.N. Sidorov, *et al.*, (Ion + molecule) equilibrium technique applied to the determination of the activities of Cr_2O_3 and NiO. Standard molar Gibbs energy of formation of $NiCr_2O_4$, *J. Chem. Thermodyn.,* 22(1990), p.623.

[12] H.W. Ng and Z. Gan, A finite element analysis technique for predicting as-sprayed residual stresses generated by the plasma spray coating process, *Finite. Elem. Anal. Des.,* 41(2005), p.1235.

[13] H.J. Yu, G.Y. Xu, X.M. Shen, *et al.*, Effects of size, shape and floatage of Cu particles on the low infrared emissivity coatings, *Prog. Org. Coat.,* 66(2009), p.161.

[14] K. Tang, R.A. Dimenna, and R.O. Buckius, Regions of validity of the geometric optics approximation for angular scattering from very rough surfaces, *Int. J. Heat Mass Transfer*, 40(1997), p.49.

[15] F. Davar, Z. Fereshteh, and M.S. Niasari, Nanoparticles Ni and NiO: synthesis, characterization and magnetic properties, *J. Alloys Compd.,* 476(2009), p.797.

[16] F. Liu., J. Lu, J. Shen, *et al.*, Preparation of mesoporous nickel oxide of sheet particles and its characterization, *Mater. Chem. Phys.*, 113(2009), p.18.

[17] M. Ocana, Nanosized Cr_2O_3 hydrate spherical particles prepared by the urea method, *J. Eur. Ceram. Soc.,* 21(2001), p.931.

[18] S.M. El-Sheikh, R.M. Mohamed, and O.A. Fouad, Synthesis and structure screening of nanostructured chromium oxide powders, *J. Alloys Compd.,* 482(2009), p.302.

[19] M. Abo-Naf, M.S. El-Amiry, and A.A. Abdel-Khalek, FT-IR and UV-Vis optical absorption spectra of γ-irradiated calcium phosphate glasses doped with Cr_2O_3, V_2O_5 and Fe_2O_3, *Opt. Mater.*, 30(2008), p.900.

[20] E. Wolska, P. Piszora, K. Stempin, *et al.*, X-ray powder diffraction study of cation distribution and the $Fd3m$-$P4_132$ symmetry reduction in $Li_{0.5}Fe_{2.5}O_4/LiMn_2O_4$ spinel solid solutions, *J. Alloys Compd.*, 286(1999), p.203.

[21] J.L. Gunjakar, A.M. More, K.V. Gurav, *et al.*, Chemical synthesis of spinel nickel ferrite ($NiFe_2O_4$) nano-sheets, *Appl. Surf. Sci.,* 254(2008), p.5844.